ChemComm

Check for updates

Statically and dynamically flexible hydrogen-bonded frameworks based on 4,5,9,10-tetrakis(4-carboxyphenyl)pyrene†

Taito Hashimoto,[a] Ryusei Oketani, [ID][ab] Asato Inoue,[a] Kohei Okubo,[c] Kouki Oka, [ID][cd] Norimitsu Tohnai, [ID][c] Kazuhide Kamiya, [ID][ab] Shuji Nakanishi [ID][ab] and Ichiro Hisaki [ID] *[ab]

Aperture shape and size of flexible hydrogen-bonded organic frameworks (HOF) were statically modulated using various aromatic solvents, and dynamically changed by desorption and adsorption of the solvent molecules.

Soft porous frameworks have been of substantial interest as the third generation of framework materials because of unique functionality provided by reversible structural changes of the frameworks.[1] Particularly, porous crystalline frameworks formed through non-covalent interactions can intrinsically show structural flexibility due to the reversible intermolecular interactions.[2] However, the structural changes often result in collapse of the periodic framework to give non-porous, less-crystalline materials.

In this context, a hydrogen-bonded organic framework (HOF)[3] is the suitable platform for flexible frameworks,[4] because of moderately directional and relatively strong H-bonding interactions.[5] For example, H. Wang and co-workers reported HOF-5 composed of a 2,4-diaminotriazine-substituted tetraphenylethene (TPE) derivative with rhombic lattice contracted by 21% upon guest removal and the resultant activated framework showed encapsulation of CO_2 with high density.[6] Z. Chi and co-workers reported a nitrobenzene-substituted TPE derivative formed framework (8PN) which shows large-scale void regulation and wide range of fluorescence color changes upon included solvent molecules.[7] More recently, some layered HOFs composed

tetracarboxylic acid derivatives were reported to undergo drastic crystal-to-crystal structural changes accompanied by rearrangements of H-bonds.[8] However, essential structural factors of flexible HOFs have remained unclear, compared to rigid HOFs.[9]

In this communication, we demonstrate that pyrene-based tetracarboxylic acid **CP-Py** forms statically and dynamically flexible HOFs with a layered structure of a **sql**-topological network (Fig. 1a). Desorption and adsorption of guest molecules triggers reversible structural transformation between **CP-Py-1** and **CP-Py-2**, the latter of which further transformed irreversibly into **CP-Py-3**. Importantly, the structures of these three forms were characterized by single crystalline X-ray diffraction (SXRD) analysis, allowing us to identify the origin of structural flexibility of the present HOFs, that is, distortion of the peripheral carboxyphenyl arms and deformation (*i.e.* twisting and bending) of the H-bonded dimer (Fig. 1b), in addition to reversible H-bond formation and dissociation (Fig. 1c). Furthermore, the crystal-to-crystal transformation was crucially supported by robust 1D columnar assembly (Fig. 1d), which allows the regulated structural changes instead of random structural changes. These results provide fundamental insight to develop a new dynamic HOF.

CP-Py was synthesized according to procedures previously reported.[10,11] **CP-Py** was dissolved in a mixed solution of DMF and 1,2-dichlorobenzene (DCB) and left the solution at 120 °C to evaporate solvent slowly, giving crystals of solvated HOF **CP-Py-1**(DCB) suitable for SXRD analysis.

CP-Py-1(DCB) has a slip-stacked, layered structure composed of hydrogen-bonded **sql**-networked sheets as reported.[11] **CP-Py-1**(DCB) included DCB molecules with a host–guest ratio of 1 : 4. Time-dependent powder X-ray diffraction (PXRD) measurements showed that diffraction peaks ascribable to **CP-Py-1**(DCB), such as those at 2θ of 12.4°, 12.9°, 17.4° and 21.1°, gradually disappeared, while new peaks at 7.6°, 12.0°, 16.9° and 21.9° appeared (Fig. 2a). This indicates that **CP-Py-1**(DCB) gradually transforms into the second crystalline form, *i.e.* **CP-Py-2**(DCB), upon spontaneous release of the solvent molecules under ambient conditions.

[a] *Division of Chemistry, Graduate School of Engineering Science, Osaka University, 1-3 Machikaneyama, Toyonaka, Osaka 560-8531, Japan. E-mail: i.hisaki.es@osaka-u.ac.jp*

[b] *Research Center for Solar Energy Chemistry, Graduate School of Engineering Science, Osaka University, 1-3 Machikaneyama, Toyonaka, Osaka 560-8531, Japan*

[c] *Department of Applied Chemistry, Graduate School of Engineering, Osaka University, 2-1 Yamadaoka, Suita, Osaka 565-0871, Japan*

[d] *Center for Future Innovation (CFi), Graduate School of Engineering, Osaka University, 2-1 Yamadaoka, Suita, Osaka 565-0871, Japan*

† Electronic supplementary information (ESI) available: Detail of experiments, TG data, PXRD data, crystal structures CCDC 2255738–2255743 and 2262072. For ESI and crystallographic data in CIF or other electronic format see DOI: https://doi.org/10.1039/d3cc01877f
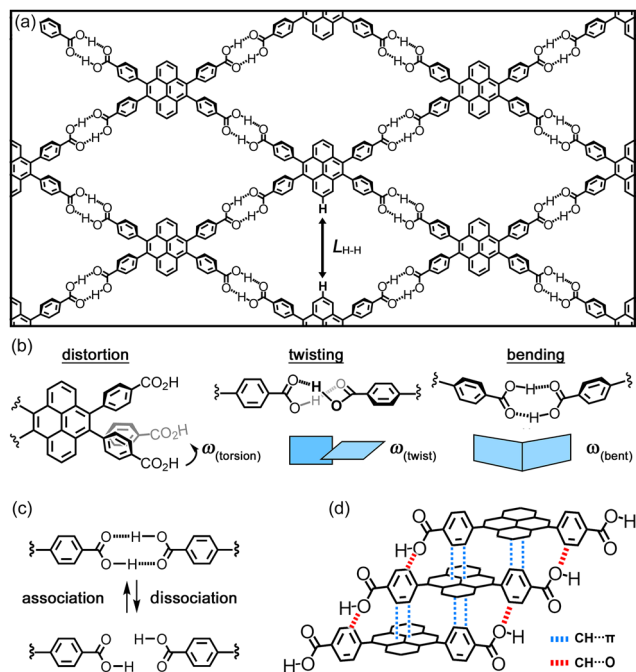
Fig. 1 Flexible H-bonded framework composed of **CP-Py**. (a) Schematic representation of the framework, where L_{H-H} denotes a distance between the diagonal aromatic hydrogen atoms of **CP-Py**. (b) Structural factors providing flexibility of the framework: distortion of the peripheral arm denoted by $\omega_{(torsion)}$ and twisting and bending of the H-bonded dimer of the carboxy groups denoted by $\omega_{(twist)}$ and $\omega_{(bent)}$, respectively. (c) Reversible H-bonding formation and dissociation. (d) Robust 1D columnar structure formed through CH···π and CH···O interactions.

It is noteworthy that addition of a drop of DCB on a bulk of **CP-Py-2**(DCB) immediately recovered the initial form **CP-Py-1**(DCB)

(Fig. S1, ESI†), allowing reversible transformation between these two phases. When **CP-Py-2**(DCB) was further left under ambient or heated conditions, the diffraction peaks ascribable to **CP-Py-2**(DCB) decayed and new peaks appeared at 9.4°, 11.2°, 13.3°, 15.5°, and 20.6°, indicating further transformation into the third form **CP-Py-3** (Fig. 2b). The thermal gravimetric curve indicates that weight loss started soon after heating and reached 45% till complete removal of the solvent at 116 °C, supporting the observed transformations accompanied by release of DCB molecules (Fig. S2, ESI†).

It was also observed that a single crystal of **CP-Py-1**(DCB) started to get cracks after wiped off bulk solvent from surface of the crystal (Fig. 2c). The cracks are nearly parallel to the (1 0 − 4) plane which corresponds to the H-bonded 2D layers (Fig. S3, ESI†). This morphological change was brought from structural transformation triggered by the solvent release. Fortunately, the resultant platelet pieces remained single-crystallinity, allowing us to reveal crystal structures of **CP-Py-2**(DCB) and **CP-Py-3** by SXRD analysis (Fig. 2d).

CP-Py-2(DCB) retains the space group of $P2_1/c$ and the H-bonded network with **sql**-topology of the original framework, while the periodicity of framework was shrunk by 4.2 Å along the shorter diagonal direction parallel to the b axis and elongated by 1.7 Å along the longer diagonal direction of the rhombic aperture, resulting decrease of inclusion spaces from 51% to 35%. **CP-Py-2**(DCB) included DCB molecules with a host–guest ratio of 1 : 2. **CP-Py-3** has a completely different molecular arrangement with the other two. H-bonded dimer of the carboxy groups expressing the graph set notation of $R_2^2(8)$ in the original rhombic framework were cleaved and re-organized by forming a distorted dimer with $R_2^2(8)$, resulting the generation of small cavity expressing the graph set notation of $R_2^2(30)$.[12] The framework of **CP-Py-3** has a
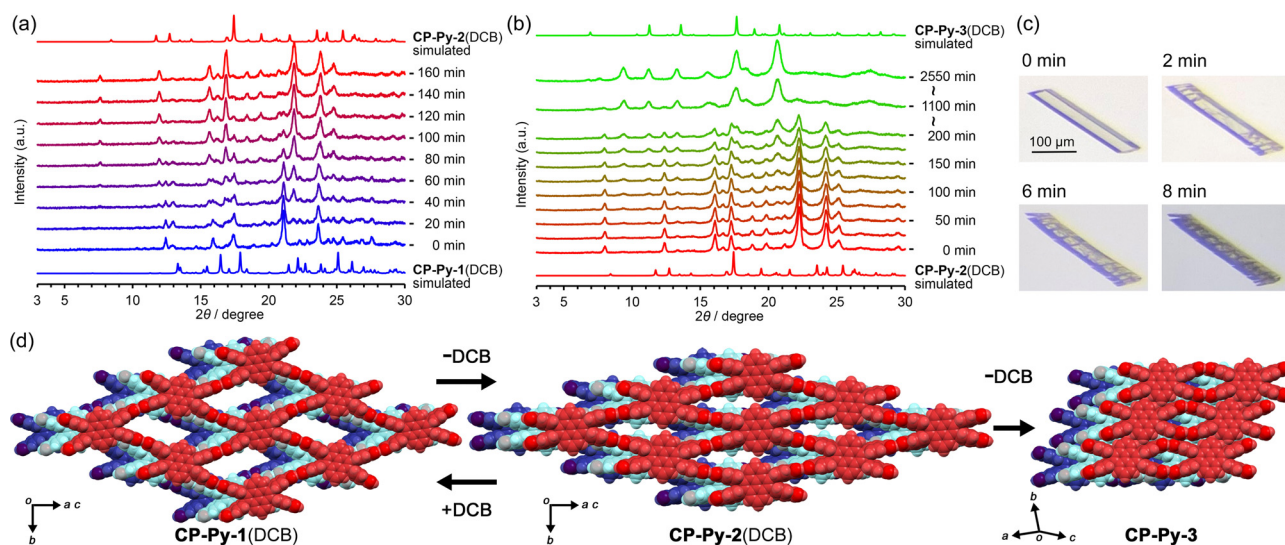

Fig. 2 Structural transformation of **CP-Py-1**(DCB) to **CP-Py-3** *via* **CP-Py-2**(DCB). (a) PXRD pattern changes from **CP-Py-1**(DCB) to **CP-Py-2**(DCB). (b) PXRD pattern changes from **CP-Py-2**(DCB) to **CP-Py-3**. (c) Morphological changes of a single crystal of **CP-Py-1**(DCB) after wiped off bulk solvent from surface of the crystal. (d) Crystal structures of **CP-Py-1**(DCB), **CP-Py-2**(DCB) and **CP-Py-3** revealed by SXRD analysis, where molecules of included DCB are omitted for clarity in the cases of **CP-Py-1**(DCB) and **CP-Py-2**(DCB). The transformation between **CP-Py-1**(DCB) and **CP-Py-2**(DCB) is reversible, while **CP-Py-3** is not able to transform neither **CP-Py-1**(DCB) nor **CP-Py-2**(DCB) without recrystallization. The simulated patterns in (a) and (b) are shifted to the wide-angle region due to temperature differences. PXRD was recorded at room temperature, while SXRD was conducted at 100 K or 113 K.

narrow bottle-necked channel with aperture dimension of 8.6 Å × 3.4 Å (Fig. S4, ESI†). The void ratio was calculated to be 12% by PLATON.[13] **CP-Py-3** was activated at 120 °C under vacuum condition and subjected to gas sorption experiments. **CP-Py-3** showed almost no N_2 adsorption, while adsorbed CO_2 with the type-I sorption isotherm (Fig. S5, ESI†), indicating existence of micro pores. Brunauer–Emmett–Teller (BET) surface area was calculated based on the CO_2 adsorption isotherm to be 172 m^2 g^{-1} (Fig. S6, ESI†). It is not negligible that CO_2 adsorption experiments reproducibly showed anomalous rapid uptake at the relative pressure larger than 0.4, indicating that sudden condensation of CO_2 occurred irregularly on surface of the crystals (Fig. S7, ESI†). Since **CP-Py-3** was formed through H-bond cleavage and rearrangements, single crystallinity was low and crystal data was not enough for detailed structural discussion.

CP-Py was, furthermore, crystallized using other aromatic solvents, such as 1,2,4-trichlorobenzene (TCB) and *N,N*-dimethylaniline (DMAni) to yield the corresponding solvated HOFs **CP-Py-1**(TCB) and **CP-Py-1**(DMAni) with host/guest ratio of 1:4 (Fig. S8–S11, ESI†). They also transform into the second forms **CP-Py-2**(TCB) and **CP-Py-2**(DMAni) upon the solvent removal (Fig. S12 and S13, ESI†), and the transformation was revealed to be reversible (Fig. S14 and S15, ESI†).

To shed a light of flexibility of the framework, the size and shape of the rhombic aperture in the obtained HOFs were compared. The structures and structural parameters are shown in Fig. 3 and Table 1, respectively. Upon transformation from **CP-Py-1**(DCB) to **CP-Py-2**(DCB), a distorted rhombic aperture with L_{H-H} distance of 7.10 Å and $\omega_{(torsion)}$ of 2.6–5.8° changed to a much narrower one with L_{H-H} of 2.65 Å and $\omega_{(torsion)}$ of 10.1–13.1°, where the molecule of **CP-Py** is forced to be deformed (Fig. 3a). **CP-Py-1**(TCB) and **CP-Py-1**(DMAni), on the other hand, have stretched similar rhombic apertures with L_{H-H} values of 6.93 Å and 8.32 Å, respectively, due to inclusion of larger solvent

Table 1 Structural parameters characterizing framework flexibility of **CP-Py**

Form	L_{H-H}/Å	$\omega_{(torsion)}{}^a$/°	$\omega_{(twist)}{}^a$/°	$\omega_{(bent)}{}^a$/°
CP-Py-1(DCB)	7.10	5.8–2.6	5.1	13.7
CP-Py-2(DCB)	2.65	13.1–10.1	11.3	3.2
CP-Py1(TCB)	6.93	4.5–3.3	3.4	3.9
CP-Py2(TCB)	2.89	9.6	0	0
CP-Py-1(DMAni)	8.32	4.3	0	0
CP-Py-2(DMAni)	5.95	9.1–2.9	3.3	16.4

^{a} Definition of the parameters are shown in Fig. S17 in ESI.

molecules (Fig. S16, ESI†). The rhombic apertures transformed into narrow and distorted ones with L_{H-H} of 2.89 Å and 5.95 Å in **CP-Py-2**(TCB) and **CP-Py-2**(DMAni), respectively, upon the solvent release. The aperture shape and shrinking manners depend on the solvent molecules included in the framework, clearly showing static and dynamic flexibility of the present framework. The flexibility was realized by distortion of the peripheral carboxyphenyl groups. The distortion angle $\omega_{(torsion)}$ of **CP-Py-1** ranges from 2.6° to 5.8° in **CP-Py-1**(DCB) and is 4.3° in **CP-Py- 1**(DMAni). Upon guest release and shrinkage of the framework, the $\omega_{(torsion)}$ values increased up to 13.1° in **CP-Py-2**(DCB). The $\omega_{(twist)}$ and $\omega_{(bent)}$, which characterize distortion in H-bonded dimer, also exhibit wide range of values depending on the aperture shape (Fig. S18, ESI†). For example, **CP-Py-1**(TCB) and **CP-Py-1**(DMAni) with stretched rhombic apertures exhibit small values of $\omega_{(twist)}$ and $\omega_{(bent)}$, while **CP-Py-1**(DCB) and **CP-Py-2**(DMAni) with distorted apertures show larger values (Table 1). It is noteworthy that addition of a drop of 1-methylnaphthalene (MeNaph) on the single crystal of **CP-Py-2**(DCB) resulted in exchange of the guest molecules from DCB to MeNaph and expansion of the framework from **CP-Py-2** to **CP-Py-1** (Fig. 4). This also clearly indicates the flexibility of the framework.
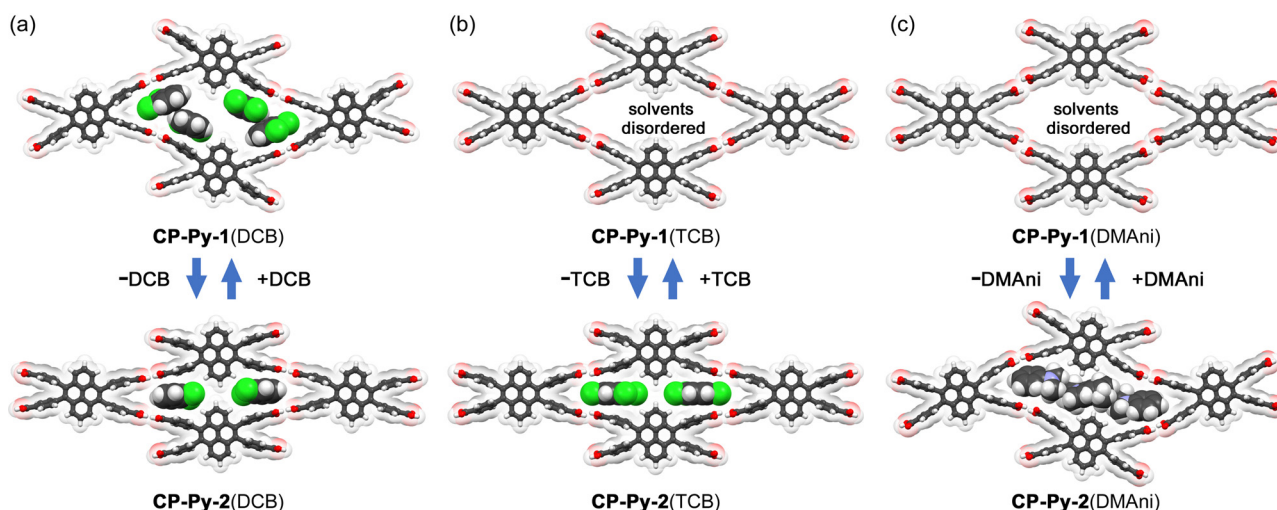

Fig. 3 Shapes of rhombic lattice changed upon partial removal of solvent molecules: (a) from **CP-Py-1**(DCB) to **CP-Py-2**(DCB), (b) from **CP-Py-1**(TCB) to **CP-Py-2**(TCB), and (c) from **CP-Py-1**(DMAni) to **CP-Py-2**(DMAni). Included solvent molecules are drawn with the space-filled model, except for those in **CP-Py-1**(TCB) and **CP-Py-1**(DMAni) which were not able to be solved crystallographically due to sever disorder. The central DMAni molecules in **CP-Py-2**(DMAni) are disordered into two positions due to the symmetry reason.
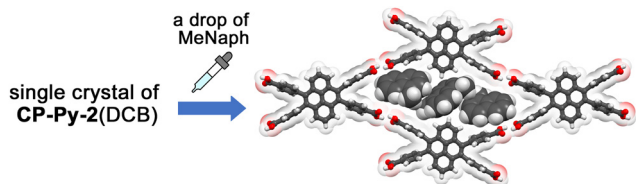
Fig. 4 Crystal-to-crystal transformation from **CP-Py-2**(DCB) to **CP-Py-1**(MeNph) by adding a drop of MeNaph on a single crystal of **CP-Py-2**(DCB).
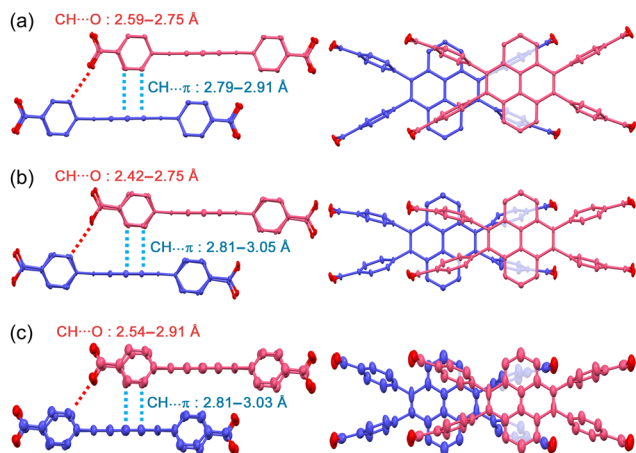

Fig. 5 Side views (left) and top views (right) of stacked two molecules of **CP-Py** in crystals of (a) **CP-Py-1**(DCB), (b) **CP-Py-2**(DCB) and (c) **CP-Py-3** The structures are drawn with anisotropic displacement ellipsoid plots with 50% probability.

Not only the flexibility of the H-bonded network structure, but robustness of the 1D stacked columnar structure also plays a role on the crystal-to-crystal structural transformation. The robust 1D columnar structure enables the framework to undergo regulated structural changes instead of random structural changes. The 1D columnar structure is formed by complementary contacts of the accumulated molecules including edge-to-face contact (*i.e.* CH···π interactions) of the peripheral phenylene groups and the central pyrene ring and the CH···O contacts of the aromatic hydrogen and the carboxy oxygen atom (Fig. 1d and 5). This contact manner is observed in all forms, and plays role to keep crystallinity, although subtle differences in rotational and conformation of the phenylene rings were observed.

In this communication, we described static and dynamic flexibility of a HOF composed of tetratopic carboxylic acid **CP-Py**. Void spaces of the framework can be statically changed upon included guest molecules. Furthermore, guest desorption and adsorption makes the framework reversibly transform between two forms **CP-Py-1** and **CP-Py-2**, the latter of which further changed into the third form **CP-Py-3** possessing permanent porosity upon complete removal of solvent molecules. All forms were successfully characterized by SXRD analysis. The present system demonstrated that both deformation-tolerant parts and structurally robust stacking part are necessary for flexible HOFs that experiences crystal-to-crystal transformation.

Conflicts of interest

There are no conflicts to declare.

Notes and references

1 (*a*) S. Kitagawa and K. Uemura, *Chem. Soc. Rev.*, 2005, **34**, 109; (*b*) S. Horike, S. Shimomura and S. Kitagawa, *Nat. Chem.*, 2009, **1**, 695; (*c*) S. Seth and S. Jhulki, *Mater. Horiz.*, 2021, **8**, 700.
2 (*a*) L. Atwood, L. J. Barbour, A. Jerga and B. L. Schottel, *Science*, 2002, **298**, 1000; (*b*) J. T. A. Jones, D. Holden, T. Mitra, T. Hasell, D. J. Adams, K. E. Jelfs, A. Trewin, D. J. Willock, G. M. Day, J. Bacsa, A. Steiner and A. I. Cooper, *Angew. Chem., Int. Ed.*, 2011, **50**, 749; (*c*) H. Yamagishi, H. Sato, A. Hori, Y. Sato, R. Matsuda, K. Kato and T. Aida, *Science*, 2018, **361**, 1242; (*d*) F. Castiglioni, W. Danowski, J. Perego, F. K.-C. Leung, P. Sozzani, S. Bracco, S. J. Wezenberg, A. Comotti and B. L. Feringa, *Nat. Chem.*, 2020, **12**, 595; (*e*) Y. Yakiyama, T. Fujinaka, M. Nishimura, R. Seki and H. Sakurai, *Chem. Commun.*, 2020, **56**, 9687.
3 (*a*) R. B. Lin, Y. He, P. Li, H. Wang, W. Zhou and B. Chen, *Chem. Soc. Rev.*, 2019, **48**, 1362; (*b*) I. Hisaki, C. Xin, K. Takahashi and T. Nakamura, *Angew. Chem., Int. Ed.*, 2019, **58**, 11160; (*c*) B. Wang, R-B. Lin, Z. Zhang, S. Xiang and B. Chen, *J. Am. Chem. Soc.*, 2020, **142**, 14399; (*d*) X. Song, Y. Wang, C. Wang, D. Wang, G. Zhuang, K. O. Kirlikovali, P. Li and O. K. Farha, *J. Am. Chem. Soc.*, 2022, **144**, 10663; (*e*) P. Li, M. R. Ryder and J. F. Stoddart, *Acc. Mater. Res.*, 2020, **1**, 77–87.
4 (*a*) I. Hisaki, S. Nakagawa, Y. Suzuki and N. Tohnai, *Chem. Lett.*, 2018, **47**, 1143–1146; (*b*) L. Chen, Z. Yuan, H. Zhang, Y. Ye, Y. Yang, F. Xiang, K. Cai, S. Xiang, B. Chen and Z. Zhang, *Angew. Chem., Int. Ed.*, 2022, **61**, e202213959; (*c*) W. Yang, W. Zhou and B. Chen, *Cryst. Growth Des.*, 2019, **19**, 5184; (*d*) Y. Suzuki, Y. Yamaguchi, R. Oketani and I. Hisaki, *Mater. Chem. Front.*, 2023, **7**, 106.
5 G. R. Desiraju, *Angew. Chem., Int. Ed. Engl.*, 1995, **34**, 2311.
6 H. Wang, B. Li, H. Wu, T.-L. Hu, Z. Yao, W. Zhou, S. Xiang and B. Chen, *J. Am. Chem. Soc.*, 2015, **137**, 9963.
7 Q. Huang, W. Li, Z. Mao, L. Qu, Y. Li, H. Zhang, T. Yu, Z. Yang, J. Zhao, Y. Zhang, M. P. Aldred and Z. Chi, *Nat. Commun.*, 2019, **10**, 3074.
8 (*a*) X.-Y. Gao, Y.-L. Li, T.-F. Liu, X.-S. Huang and R. Cao, *CrystEngComm*, 2021, **23**, 4743; (*b*) Q. Ji, K. Takahashi, S. Noro, Y. Ishigaki, K. Kokado, T. Nakamura and I. Hisaki, *Cryst. Growth Des.*, 2021, **21**, 4656; (*c*) H. Kubo, R. Oketani and I. Hisaki, *Chem. Commun.*, 2021, **57**, 8568.
9 (*a*) F. Hu, C. Liu, M. Wu, J. Pang, F. Jiang, D. Yuan and M. Hong, *Angew. Chem., Int. Ed.*, 2017, **56**, 2101; (*b*) I. Hisaki, N. Ikenaka, E. Gomez, B. Cohen, N. Tohnai and A. Douhal, *Chem. – Eur. J.*, 2017, **23**, 11611; (*c*) Q. Yin, P. Zhao, R.-J. Sa, G.-C. Chen, J. Lg, T.-F. Liu and R. Cao, *Angew. Chem., Int. Ed.*, 2018, **57**, 7691; (*d*) I. Hisaki, Y. Suzuki, E. Gomez, B. Cohen, N. Tohnai and A. Douhal, *Angew. Chem., Int. Ed.*, 2018, **57**, 12650.
10 Z. Lu, R. Wang, Y. Liao, O. K. Farha, W. Bi, T. R. Sheridan, K. Zhang, J. Duan, J. Liu and J. T. Hupp, *Chem. Commun.*, 2021, **57**, 3571.
11 T. Hashimoto, R. Oketani, M. Nobuoka, S. Seki and I. Hisaki, *Angew. Chem., Int. Ed.*, 2023, **62**, e202215836.
12 J. Bernstein, R. E. Davis, L. Shimoni and N.-L. Chang, *Angew. Chem., Int. Ed. Engl.*, 1995, **34**, 1555.
13 A. L. Spek, *Acta Crystallogr., Sect. D: Biol. Crystallogr.*, 2009, **65**, 148.